RSC Advances

ROYAL SOCIETY OF CHEMISTRY

www.rsc.org/advances

The table of contents

Direct Printed Silver Nanowire Thin Film Patterns for Flexible Transparent Heaters with Temperature Gradient

*Po-Hsuan Wang, Shih-Pin Chen, Chun-Hao Su and Ying-Chih Liao**

Silver nanowire thin film patterns are printed precisely to form transparent heaters with uniform or gradient temperature distributions.

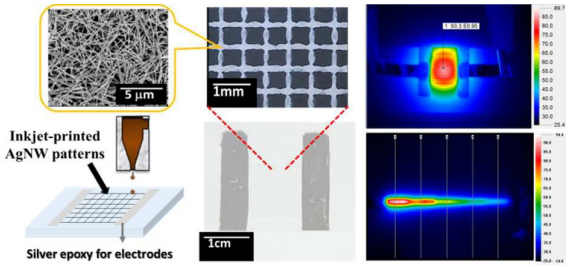

Journal Name

ARTICLE

Direct Printed Silver Nanowire Thin Film Patterns for Flexible Transparent Heaters with Temperature Gradient

Received 00th January 20xx,
Accepted 00th January 20xx

DOI: 10.1039/x0xx00000x

www.rsc.org/

Po-Hsuan Wang,[a] Shih-Pin Chen[a] Chun-Hao Su[a] and Ying-Chih Liao[a*]

In this study, a convenient and facile direct printing method is developed to fabricate patterned silver nanowire (AgNW) thin films. An aquesous silver nanowire (AgNW) ink was first formulated and inkjet printed on flexible substrates with precisely controlled AgNW density per unit area. With a mesh grid structure, the printed heater showed high electrical conductivities with great transparency up to 90%. From infrared thermography, a steady-state temperature up to 100°C with merely 4 volt applied voltage was observed uniformly over the printed mesh grid heater. With great control on local resistances via AgNW density variation, a gradient heater was designed and printed directly to provide a temperature gradient up to 10°C/cm. When printed on thin polyethylene terephthalate (PET) sheets, the printed heater can have a fast response time within 3 s due to the thermal insulting nature of PET. The printed heaters on PET also showed great mechanical stability and the resistances remained almost the same after 1000 bending cycles.

Introduction

Transparent heaters have attracted uprising interest for its wild applications including defrosters[1], displays[2], solar panels[3] and touch screens[4]. The principle of electrical heaters is based on Joule heating, which convert electricity to heat through the resistive losses. The power dissipated in a resistive conductor can be described by Joule's first law: $P = V^2/R$, where V is the applied voltage and R is the total resistance. A low resistance is regularly necessary to obtain high heating powers at low applied voltages to prevent electrical damages of electrical devices or shocks to human body. The most commonly used material for transparent heaters is indium tin oxide (ITO), which possesses high optical transparency (~90%) and low sheet resistance (<100 Ω/□). However, due to the brittleness of ITO, the heaters made of ITO have a low tolerance to external stresses and thus little flexibility. To meet the surging demands of flexibility and portability in the next-generation macroelectronic systems, recent researches focus on the development of new transparent conductive materials with better mechanical strength, such as conducting polymers, [5, 6] carbon nanotubes (CNTs),[7, 8] graphene,[9, 10] and metallic nanowires.[11, 12] Among them, silver nanowire (AgNW) thin films demonstrate both low sheet resistance and great optical transparency from its percolating structure.[13, 14] Moreover, the network structures of AgNW also allows great flexibility to accommodate external mechanical stresses.[15] Thus, AgNW have been widely used in transparent heaters.[16]

To fabricate flexible AgNW thin film heaters with great electro-optical properties, it is necessary to develop simple, reliable and cost effective coating techniques. To fulfil these requirements, solution-process techniques operated at room temperature, such as spray coating[17], bar coating,[18] or vacuum filtration,[1, 12] have been commonly used. These wet coating methods can be easily scalable to produce AgNW thin films with arbitrarily large areas. With these methods, large-area AgNW thin film heaters with uniform temperature profiles and high optical transparency have been reported (Table 1). On the other hand, for biomedical applications, such as PCR & microfluidic devices,[19, 20] local temperature gradients are usually needed for proper biochemical reaction conditions. Moreover, transparency is also necessary for these microfluidic applications with cell observation.[21] To fabricate these patterned thin film heaters with both great local temperature control and transparency to achieve various temperature distributions, commonly used coating techniques combined with pre-defined masks can be applied[22] but with vast amount of material wastes.

Inkjet printing technology, a direct-writing method which can precisely control liquid deposition effectively for patterns, is commonly used to fabricate electronic devices in the literature.[23] However, due to the nozzle clogging problem caused by the large aspect ratio of AgNWs, only a few reports are available for applying inkjet printing process on pristine AgNW pattern fabrication in the literature. Wu et al[24] first combined the AgNW with silver nanoparticles for inkjet printing, and the results showed that the addition of AgNW can effectively decrease the sheet resistance of printed thin films. Later, Lu et al. printed AgNW thin films for

[a] Department of Chemical Engineering, National Taiwan University, Taipei, 10615, Taiwan

Address correspondence to Ying-Chih Liao, E-mail: liaoy@ntu.edu.tw

Electronic Supplementary Information (ESI) available: [details of any supplementary information available should be included here]. See DOI: 10.1039/x0xx00000x

organic photovoltaic devices.[25, 26] Finn et al.[27] further improved the system using the single phase AgNW solution to fabricate conductive thin film without high temperature sintering. These pioneer researches show the possibility to control the local resistance of 1-D nanomaterials such as AgNW. Based on these researches, a modified aqueous AgNW ink[28] was recently formulated for inkjet printing process without any additive to fabricate transparent optoelectronic devices. In this study, with appropriate pattern designs and precise control of AgNW deposition, transparent thin film heaters will be inkjet-printed to demonstrate efficient heating for either uniform or gradient temperature profiles. The characteristics of the printed heaters, such as heating powers and response times, will be carefully examined to investigate the performances of the printed heaters.

Experimental

Materials

Ethanol and acetone were purchased from Sigma-Aldrich, USA. Deionized water (Millipore Milli-Q grade) with resistivity of 18.2 $M\Omega cm^{-1}$ was used in this experiment. Silver nanowire (AgNW, 0.5 wt%) in isopropanol with diameter of 120 nm and length of 3~5 μm was supplied by Emfutur, Spain. Flexible polyethylene terephthalate (PET) slides of 25 μm thickness was purchased from Nanya plastics, Taiwan. Glass slides with 1mm thickness were purchased from FEA, Taiwan. Silver paste was purchased from Fujikura Kasei, Japan.

AgNW ink preparation

First, acetone was added in AgNW dispersion in a 1:1 volume ratio. The mixture was then put in a centrifuge (Z206A, Hermle) at 1500 RPM for 15 minutes for AgNW sedimentation. After centrifugation, the supernatant solvent was removed and the sediment was dried slightly at room temperature. The wet AgNW sediment containing little acetone amount was then mixed in deionized water to form a 0.8 mg/ml aqueous solution. To obtain stable AgNW suspension, the AgNW ink was sonicated in ultrasonic bath (DC300H, DELTA) for 30 minutes at 20 °C. The viscosity of AgNW ink was 0.92 cp at 20 °C, measured by Brookfield DV-III Ultra Rheometer. Contact angles of the prepared AgNW ink, measured by an in-house goniometer, were 58 and 50 degrees on glass and PET, respectively.

Fabrication and characterization of AgNW thin film patterns

Glass and PET substrates were first rinsed sequentially with water and ethanol, and then dried in a vacuum oven at 60 °C. A piezoelectric inkjet printer (JetLab4, MicroFab, USA) was utilized to print the aqueous AgNW ink. Droplets of 70 μm in diameter were ejected consistently from a 50 μm nozzle at a velocity of 5 m/s. The substrates were put on a heating stage with an operating temperature of 45°C. After printing, the printed AgNW patterns, which dried on the heating stage, were connected with copper tapes by gluing with silver paste for power connection. Heating performances of the printed AgNW heaters were measured by an IR microscope (Ching Shing Computer-Tech, Taiwan). SEM images were carried out using Nova NanoSEM 230 (FEI Company, USA). The electrical resistance of the printed patterns was measured by a multimeter (HOLA, DM-2690TU) with two-point mode. The UV spectra of the printed heaters were collected by UV spectrometer (DH- 2000-BAL, USA).

Results and discussion

Resistance of AgNW conductive tracks

Acording to Joule heating effect, the electrical resistances of the printed devices can directly determine the heating power. As shown in the literature,[29] the major resistance of AgNW thin films comes from the contact resistance between nanowires. Thus, with increasing AgNW densities, the better percolation in AgNW thin films can greatly reduce the electrical resistance. The relationship between the AgNW density and electrical resistance is thus very important to the heater designs. To precisely control the density of the printed patterns, an inkjet printing approach with multiple passes is used here. First, the resistances of straight lines, printed with a dot-to-dot spacing of 45 μm, are recorded (Fig. 1). Because of the low AgNW density (0.8 mg/mL), multiple printing layers are needed to create effective AgNW percolation for conductive straight lines. As shown in Fig. 1(a), after deposit for 20 layers, the printed line has an average line width of 100 μm. The low concentration leads to non-uniform thin film,

Table 1 Comparison of AgNW-based thin film heaters

Coating Method	Materials	Input	Max. Temp. (°C)	T%	Substrate	Process Temp. (°C)	Rs (Ω/sq)	t_{res}(s)
Vacuum filtration[1]	GO/AgNW	15V	210	80	Quartz	700	27	110
Vacuum filtration[12]	AgNW	7V	140	92	PET	R.T.	11	140
Spray[11]	AgNW	7V	55	90	PEN	80	35	100
Spray[30]	AgNW	100 mA	48	61	PET	120	15	100
Bar coating[15]	AgNW	7V	105	90	PET	100	10	45
Roll to roll[31]	CNT/AgNW	15V	105	95	PET	100	30	15
this work	AgNW	4 -15V	102	65-90	PET or glass	45	-	3

as observed from the white clusters inside the printed thin films and some coffee ring effects around the line edges. Because of the little AgNW amount, a layer of AgNWs with few contact points (Fig. 1(b)) is formed. Due to less effective contacts, the printed lines, which has a length of 1 cm, has a quite large resistance of around 2000 Ω/cm. As one increases the number of printing layers, the AgNW density increases and the printed lines show a more solid white colour under microscope with nearly no coffee ring effects. The more AgNW densities also leads to better nanowire percolation and thus the resistance drops quickly to ~300 Ω/cm with 40 printing layers (Fig. 1(c)). As the number of layers keeps increasing, the SEM images (Fig. 1(b)) indicate that dense AgNW layers with great nanowire percolations are formed for those lines made by printing more than 60 layers. Thus, the resistance of the printed lines decreases slowly after 60 printing layers. This experiment shows that the electrical resistance of conductive patterns can be adjusted with the assistance of inkjet printing and one can easily fabricate patterns with different local resistances by controlling the deposited AgNW amounts.

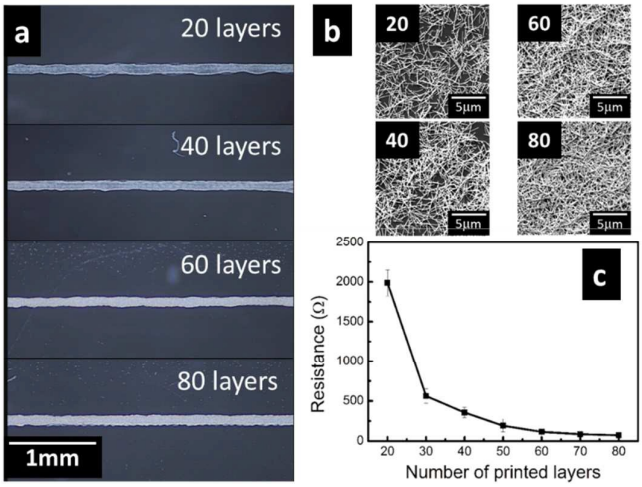

Fig. 1 (a) Optical microscopic images of the printed AgNW straight lines on glass with various printing layers. (b) The SEM images of the printed lines in (a). The increase in AgNW density with increasing printing layers shows a better percolating network. (c) Relationship between printing layers and resistance of AgNW track (1cm long).

Mesh Grid Heaters

The inkjet printing process can be applied easily to digitally print conductive mesh grids to provide uniform heating over a certain area. In the literature, most of the AgNW-based thin film heaters are composed of a uniform AgNW layer with a low sheet resistance of less than 100 Ω/□.[15] From Joule's law and Ohm's law:

$$P = IV = I^2R = \frac{V^2}{R} \qquad (1)$$

one can expect that lower resistance can lead to a better electro-thermal power. Moreover, because the AgNW percolating network allows light penetration, AgNW thin film heaters usually have high transparency ranging from 80% to 98% [1, 11, 12, 15, 30, 31] (Table 1). However, printing AgNW over an area with multiple passes can be quite time-consuming. Thus, to create a heater covering large areas with reasonable transparency, here a mesh grid is inkjet-printed to increase the heater transparency and show the capability of inkjet printing technology for well-defined printing patterns. As shown in Fig. 2, a mesh grid composed of 21×21 printed conductive tracks is printed over a 1 cm × 1 cm area on a glass slide with both good electrical conductivity and optical transparency. Because the grid structure has a large ratio of open area (about 64%), the transparency of the whole device can reach up to 90% (Fig. 2(b)) over the visible light range (450-750 nm) with low electrical resistances. With more layers printed, the transparency decreases slowly down to 67% at 30 layers. This value is quite close to the open area ratio of 64%, and shows the strong light shielding effect at large printed AgNW amounts, as indicated by Finn et al.[27]

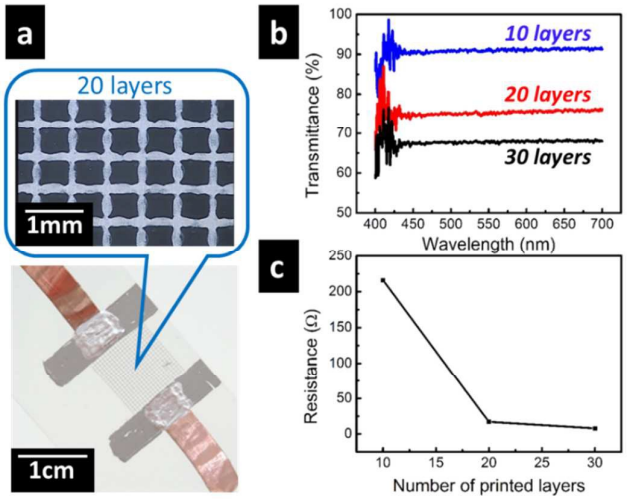

Fig. 2 (a) Optical microscopic images of a printed AgNW mesh (20 layers) on a glass slide. Two sides of the printed mesh are connected to copper tape with silver paste. Variation of (b) optical transmittance and (c) electrical resistance with number of layers for printed AgNW meshes. All the meshes were composed of 21 lines (~ 100 μm line width) with a line pitch of 500 μm to cover a 1 cm×1 cm area.

In contrast to single conductive tracks, the overall resistance of the printed mesh grid between the two silver paste electrodes decreases drastically due to the grid structure. Because the tracks parallel to the silver paste electrodes ensure the connection between the vertical tracks, the equivalent resistance R_{eq} of the printed mesh grids is 15 Ω with 20 layers, much lower than the resistance of a single track (2000 Ω) of 1 cm. The low resistance thus leads to a great heating power (Fig. 3). From the thermographs, the printed mesh heater with 20 layers of the AgNW ink can reach up to 93°C with an input voltage of merely 4V, which is quite good compared to others (Table 1). The mesh heater also provides a uniform heating over a circular area of ~ 1 cm diameter, possibly due to the isotropic heat dissipation. The response

time (~200s) for the heater to reach equilibrium temperature, however, is somewhat slower than those in the literature (Table 1). This slow response time is due to the large thermal capacity of the substrate, and will be discussed in a later section.

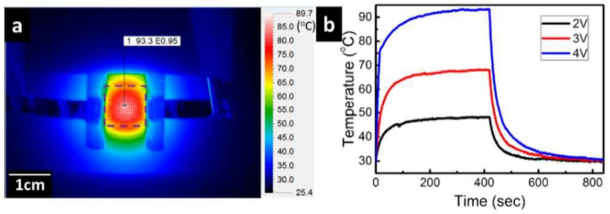

Fig. 3 (a) Infra-red image of the AgNW mesh on a glass slide under 4V input voltage for 400s. The mesh grid heater, indicated by the square of mesh lines, was printed with 20 layers. (b) Transient temperature profiles at the central point (as pointed in (a)) of the AgNW mesh with different input voltages.

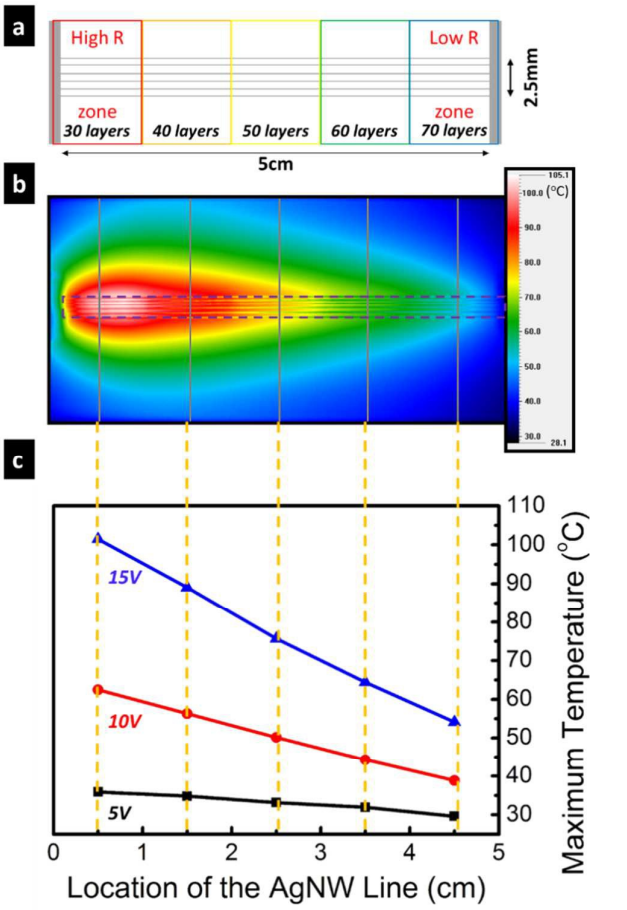

Fig. 4 (a) Pattern design of a gradient heater on glass: the local resistance was controlled by printing different layers of AgNW lines. (b) IR image of the AgNW gradient heater under 15V input voltage after 400 s. (c) The temperature distribution along the printed tracks extracted from IR images.

Gradient Heater

Besides heating uniformly within an area, one can also fabricate heaters with local or gradient heating effects. Fig. 4(a) shows a simple design that can yield in temperature gradient. The pattern consists of six 5-cm-long AgNW tracks in parallel with a line pitch 0.5 mm apart on glass. In each track, different thicknesses, 30-70 printing layers for each centimetre, are deposited to create a gradient (or step) resistance decrease. Because current through each single track remains the same for each zone, the highest temperature occurs at the location with highest resistance, where the heating power $P=I^2R$ is the highest (Fig. 4(b)). A large gradient of 10 ^{o}C/cm can be generated with a 15V input voltage: the temperature drops quickly from 100 ^{o}C to 60 ^{o}C within 4 cm (Fig. 4(c)). By employing different voltages, the gradient of the temperature distribution can also be adjusted as well. At an applied voltage of 5 V, the temperature gradient drops down to 1.25 ^{o}C/cm. Based on these observation, one can also adjust the temperature gradient easily by varying the heating zone lengths (here 1 cm for each zone is used) or by manipulating the AgNW density difference in each zones. Computer simulations can also be used to help designing the AgNW patterns for specific thermal gradients.

Response time

The other important issue of a heater is the response time (t_{res}). A good heater should be able to reach high temperature in a short time period after applying electrical power. In the case of heaters on the glass slide, the heat dissipation is huge due to the large heat capacitance of 1 mm thick glass. To heat up the glass slide underneath the heater, one can roughly estimate the time scale from energy balance between electrical power and heat loss into the substrate:

$$P\, t_{res} \sim \rho C_p A\, t\, \Delta T \qquad (2)$$

where ρ is the density, C_p is the specific heat capacity, A is the heating area, t is the thickness of the substrate, and ΔT is the temperature difference at equilibrium. To reduce the heat loss in the substrate and further improve the response time, a thin PET substrate is used here. Using the physical properties given in Table 2 and Eq. (2), the response time t_{res} can roughly reduce by 28 times with the PET sheet, assuming the heating area A is the same. However, as shown in Fig. 5(d), the response of the same gradient heater on the PET sheet is quite fast and has a t_{res}~ 3 s, about 60 times faster than that on glass. This discrepancy happens simply because the thermal diffusion in glass is larger, and thus leads to a larger heating area. As shown in Fig. 5(b), the heating area on PET is nearly restricted to the area around the printed heater, due to its low thermal conductivity, while the heat can diffuse to the surrounding glass substrate within about 3 times larger area. Therefore, the response time on glass actually is longer than expected by using the designed heater area.

Table 2 Physical properties of substrates

	Density (kg/m^3)	Specific heat capacity (J/kg/K)	Thickness (mm)	Thermal conductivity (W/mK)
Glass	2400	500	1	1.05
PET	1380	1250	0.025	0.18

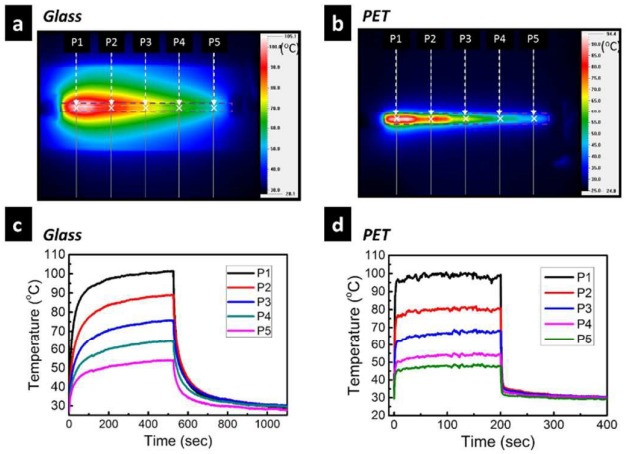

Fig. 5 (a)(b) IR image of the AgNW gradient heater on glass and PET under 15V input voltage. (c)(d) P1 to P5 temperature profiles (cross marked position in (a)(b)) of the AgNW gradient heater on glass and PET as a function of time at 15V input.

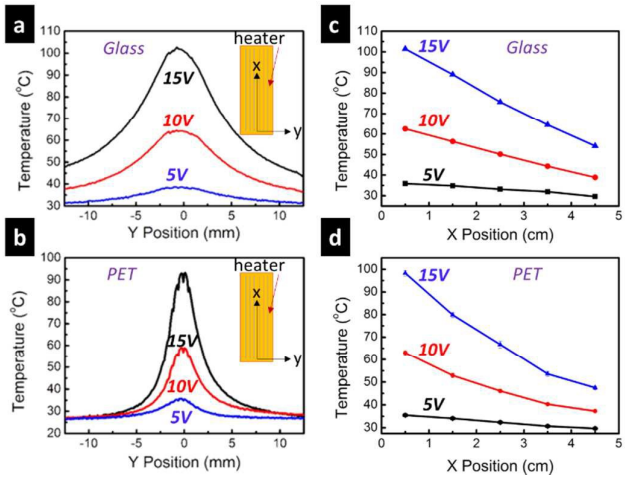

Fig. 6 The temperature distribution along y-axis for printed heaters on (a) glass slides and (b) PET sheets. The x position of the sampling point is the same as point P1 in Fig. 5(a). The steady-state temperature distribution along x-axis at different input voltages for (c) glass and (d) PET, respectively. These line plot data are extracted from the IR image analyses similar to Fig. 5 (a) or 5(b)

Heat dissipation

The diffusional heat transfer around the heaters on various substrates can be roughly estimated by comparing the thermal conductivity k. Because PET has a much lower thermal conductivity, i.e., PET is a better heat insulating material than glass, the heat diffusion is expected to be little cross sectional direction (y-direction in Fig. 6(a)). With an applied voltage of 5 V, the steady-state temperature across the heated glass slide decreases slowly from the heater printed at the center and affects almost all the slide area (the slide has a width of 2.5 cm). In contrast, as depicted in Fig. 6(b), the temperature decreases sharply from the along the y-axis on PET and only affects ~ 5 mm in width. As the applied voltage increases, the temperature profiles on PET becomes wider in y-direction because of higher power input or higher heater temperatures. At the same time, the affected width of the heaters on glass slides remains almost the same regardless of the applied voltage, possibly due to it high thermal conductivity. On the other hand, along the x-axis of the printed heater, the temperature profiles of the heaters are nearly the same for both glass and PET (Fig. 6(c-d)), possibly because of the same power input and convective dissipation to the air at steady state. These observations shows the importance of the thermal conductivity of the substrates on the temperature distributions. Thus, to apply these heaters for a restricted patterned area, such as a microfluidic channel, one should select the substrate carefully according to their insulating ability.

Mechanical Stability and Critical Applied Voltage

The printed AgNW tracks on PET show great mechanical stability. As shown in Fig. 7, the resistance of the heater remains nearly the same after bending for 500 times, but starts to slightly increases after 1000 times. Nevertheless, the resistance changes only by 8% after 5000 times, and the heating performance of the mesh heater remain functional with roughly the same temperature profiles in Fig. 3. The maximum operating voltage of the heater, or the highest heater temperature, however, is determined by the nature of AgNW. Because the nanowires have a small radius, the melting temperature is much lower than that of bulk silver.[32] As depicted in Fig. 8, when the AgNW thin films are heated, the AgNWs start to melt at around 200°C, and the printed heaters can fail if the local temperature exceeds this critical value. For the heaters on flexible PET substrates, because of the low glass transition temperature (~70°C), this critical temperature is rarely reached. However, if a high temperature larger than 150°C is required, there could be a constraint for AgNW-based heaters. Because the thin films are made of percolating nanowires, in which electric currents pass through, the temperature of the AgNW can be higher than the measured or bulk temperatures of the substrates. The narrow cross sectional areas of nanowires can yield in high local current, and the resulted heat can lead to nanowire fusion. A typical example is demonstrated in Fig. 8(c). A mesh heater made by printing 10 layers is printed on a glass slide to provide a uniform heating. The heater works well with an operating voltage of 10 V to

provide a steady-state temperature of 70 °C. As one increases the voltage to 15V for higher temperature requirement, the temperature increases to 120 °C in ~200 s, and suddenly drops. After the failure, the heater shows a much larger resistance. The damaged heater is examined carefully under SEM, and the microstructure shows fused AgNWs over several printed tracks (Fig. 8(d)). This solid evidence indicates that the real temperature of AgNWs can be much higher than the measured temperature from the IR microscope, which only provide a best resolution of ~ 10 micrometers.

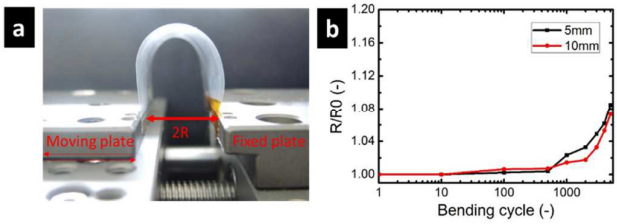

Fig. 7 (a) The setup of bending tests. (b) Durability test of AgNW mesh heater with different bending radius for 5000 times of bending cycles.

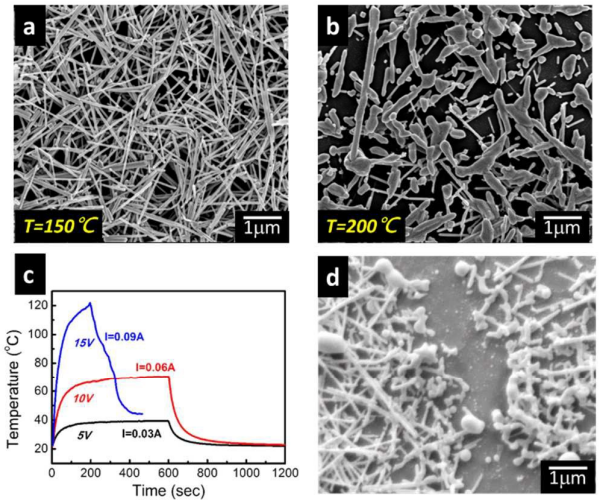

Fig. 8 SEM images for printed AgNW thin films (40 layers) heated on a hotplate for an hour at (a) 150 °C, (b) 200 °C. (c) Thermal response of a mesh heater (10 layers) on a glass slide at various applied voltages. (d) The SEM image of the damaged heater in (c) after applying 15V for 500 s.

Conclusions

A simple strategy is developed to directly print conductive silver nanowire patterns for transparent thin film heaters. In contrast to other large-area deposition methods in the literature, the inkjet printing method provides an effective solution for heater designs, including local heating, gradient heating, and uniform heating as well. The number density of AgNW per unit area can be precisely controlled, and the printed heaters possess both great optical transparency (up to 90%) and strong mechanical durability on flexible substrate without post sintering treatment. By varying the printed AgNW density, a large temperature gradient up to 10 °C/cm can be obtained. With careful selection of printing substrates, the printed heater can have a fast response (~3 sec) to the input voltages. Due to the nanoscale nature of AgNW, however, this approach can only provide heating temperatures lower than 200°C. In summary, this study illustrates the feasibility of applying inkjet printing process to produce arbitrary thin film patterns with 1-D nanowire material, and the developed inkjet printing technology can be further integrated with other microfluidic applications.

Acknowledgements

The authors are grateful to Ministry of Science and Technology (MOST) of Taiwan for supporting this research.

References

1 X. Zhang, X. Yan, J. Chen, and J. Zhao, *Carbon*, 2014. **69**. 437-443.
2 S. Bae, H. Kim, Y. Lee, X. Xu, J.-S. Park, Y. Zheng, J. Balakrishnan, T. Lei, H. Ri Kim, Y.I. Song, Y.-J. Kim, K.S. Kim, B. Ozyilmaz, J.-H. Ahn, B.H. Hong, and S. Iijima, *Nat Nano*, 2010. **5**(8). 574-578.
3 M.G. Kang, T. Xu, H.J. Park, X. Luo, and L.J. Guo, *Adv. Mater.*, 2010. **22**(39). 4378-83.
4 S. Pang, Y. Hernandez, X. Feng, and K. Müllen, *Adv. Mater.*, 2011. **23**(25). 2779-2795.
5 S. Ji, W. He, K. Wang, Y. Ran, and C. Ye, *Small*, 2014. **10**(23). 4951-60.
6 W. Hong, Y. Xu, G. Lu, C. Li, and G. Shi, *Electrochemistry Comm.*, 2008. **10**(10). 1555-1558.
7 T.J. Kang, T. Kim, S.M. Seo, Y.J. Park, and Y.H. Kim, *Carbon*, 2011. **49**(4). 1087-1093.
8 H.-S. Jang, S.K. Jeon, and S.H. Nahm, *Carbon*, 2011. **49**(1). 111-116.
9 J. Kang, H. Kim, K.S. Kim, S.K. Lee, S. Bae, J.H. Ahn, Y.J. Kim, J.B. Choi, and B.H. Hong, *Nano Lett.*, 2011. **11**(12). 5154-8.
10 H. Woo Kim, S. Jea Park, B.-K. Lee, and D. Sung Kim, *Appl. Phys. Lett.*, 2013. **102**(10). 101907.
11 C. Celle, C. Mayousse, E. Moreau, H. Basti, A. Carella, and J.-P. Simonato, *Nano Research*, 2012. **5**(6). 427-433.
12 S. Wang, X. Zhang, and W. Zhao, *J. Nanomaterials*, 2013. **2013**. 6.
13 S. De, T.M. Higgins, P.E. Lyons, E.M. Doherty, P.N. Nirmalraj, W.J. Blau, J.J. Boland, and J.N. Coleman, *ACS Nano*, 2009. **3**(7). 1767-1774.
14 S. De, P.J. King, P.E. Lyons, U. Khan, and J.N. Coleman, *ACS Nano*, 2010. **4**(12). 7064-7072.
15 T. Kim, Y.W. Kim, H.S. Lee, H. Kim, W.S. Yang, and K.S. Suh, *Adv. Funct. Mater.*, 2013. **23**(10). 1250-1255.
16 L. Daniel, G. Gaël, M. Céline, C. Caroline, B. Daniel, and S. Jean-Pierre, *Nanotechnology*, 2013. **24**(45). 452001.
17 T. Kim, A. Canlier, G.H. Kim, J. Choi, M. Park, and S.M. Han, *ACS Appl. Mater. Interfaces*, 2013. **5**(3). 788-94.
18 C.H. Liu and X. Yu, *Nanoscale Res. Lett.*, 2011. **6**(1). 75.
19 K.-C. Li, S.-T. Ding, E.-C. Lin, L. Wang, and Y.-W. Lu, *Biomicrofluidics*, 2014. **8**(6). 064109.

20 V. Miralles, A. Huerre, F. Malloggi, and M.-C. Jullien, *Diagnostics*, 2013. **3**(1). 33-67.

21 I.F. Yu, Y.H. Yu, L.Y. Chen, S.K. Fan, H.Y.E. Chou, and J.T. Yang, *Lab Chip*, 2014. **14**(18). 3621-3628.

22 A. Ohlander, C. Zilio, T. Hammerle, S. Zelenin, G. Klink, M. Chiari, K. Bock, and A. Russom, *Lab Chip*, 2013. **13**(11). 2075-82.

23 S.P. Chen, H.L. Chiu, P.H. Wang, and Y.C. Liao, *ECS J. Solid State Sci. Tech.*, 2015. **4**(4). P3026-P3033.

24 J.-T. Wu, S. Lien-Chung Hsu, M.-H. Tsai, Y.-F. Liu, and W.-S. Hwang, *J. Mater. Chem.*, 2012. **22**(31). 15599.

25 H. Lu, J. Lin, N. Wu, S. Nie, Q. Luo, C.-Q. Ma, and Z. Cui, *Appl. Phys. Lett.*, 2015. **106**(9). 093302.

26 L. Yang, T. Zhang, H. Zhou, S.C. Price, B.J. Wiley, and W. You, *ACS Appl. Mater. Interfaces*, 2011. **3**(10). 4075-4084.

27 D.J. Finn, M. Lotya, and J.N. Coleman, *ACS Appl. Mater. Interfaces*, 2015. **7**(17). 9254-9261.

28 S.-P. Chen, J.R. Durán Retamal, D.-H. Lien, J.-H. He, and Y.-C. Liao, *RSC Adv.*, 2015. **5**(87). 70707-70712.

29 Z. Siwei, G. Yuan, H. Bin, L. Jia, S. Jun, F. Zhiyong, and Z. Jun, *Nanotechnology*, 2013. **24**(33). 335202.

30 S. Sorel, D. Bellet, and J.N. Coleman, *ACS Nano*, 2014. **8**(5). 4805-4814.

31 D. Kim, L. Zhu, D.-J. Jeong, K. Chun, Y.-Y. Bang, S.-R. Kim, J.-H. Kim, and S.-K. Oh, *Carbon*, 2013. **63**. 530-536.

32 B.-T. Liu and S.-X. Huang, *RSC Adv.*, 2014. **4**(103). 59226-59232.